Prestressing Effect on Continuous Reinforced Concrete Beams Strengthened Against Shear

Dr. Hayder H. H. Kamonna*

Abstract— The present study deals with the nonlinear finite element analysis of continuous reinforced concrete (RC) beam strengthened by carbon fiber reinforced polymer (CFRP) sheet against shear. Normal and high strength concrete are investigated. ANSYS V15 program has been used to achieve the present work. Nine beams have been studied. For some beams, longitudinal CFRP sheets have been suggested to be added to study the effect of prestressing on the beam response. Different levels of prestressing have been applied. Also the position and length of such sheets have been considered to determine the best configuration.

It is found that increasing prestressing force ratio up to 50% results in an increment in cracking and ultimate loads to about 86% and 36%, respectively. It is also obtained that changing the length of prestressing CFRP sheets in the bottom face of beam (in the positive moment region) has more effect than those in the top face (in the negative moment region). Finally, it is concluded that the prestressing CFRP sheets do not prefer to be extended beyond the inflection points to achieve an improvement in cracking and ultimate loads.

Index Terms— Shear Strength, Reinforced Concrete Continuous Beam, Carbon Fiber, Strengthened, Nonlinear Finite Element Analysis

1 INTRODUCTION

Strengthening of structure may be required for different reasons. Among of these reasons are: an implementation of additional services or mistakes in the design or construction, or change in function, or to repair damage. There are different strengthening techniques. Repeatedly applying is externally bonded reinforcement (EBR), established on fiber reinforced polymers (FRP), which called FRP EBR (Taerwe et al. 2009).

Below some literatures published about behavior of continuous reinforced concrete beams strengthened by FRP EBR for shear, flexure or both.

Grace (2001) through an investigation the strengthening of continuous beams for shear and flexure using CFRP strips found that CFRP strips were not stressed to their maximum capacity when the beams failed, which led to ductile failures in all the beams. For some beams (designed to fail in flexure), flexural capacity was increased by 40%. The other beams (designed to fail in shear) showed an improvement in shear capacity by 29%.

Ashour et al. (2004) detected that there are three major modes in flexural failure. These are laminate rupture, laminate separation and peeling failure of the concrete cover attached to the composite laminate. It is found that the ductility of all strengthened beams was reduced compared with that of the respective unstrengthened control beam.

Taerwe et al. (2009) were found that FRP strengthened cross-sections limit the rotation of a plastic hinge at that location, and permit additional plastic hinge formation in strengthened one. They were also recognized that the debonding mechanisms are also governed by the moment redistribution and shear force happening in multi-span beams.

Maghsoudi and Bengar (2009) investigated the responses of reinforced high strength concrete RHSC continuous beams. Thickness of (CFRP) sheets, strengthening of both the positive and negative moment region, and end anchorage technique were the main parameters examined. It was concluded that increasing the number of CFRP sheet layers increases ultimate strength, and reduces ductility. Also, using end anchorage increases ultimate strength.

Jumaat et. al (2010) proposed a simple method of applying CFRP for strengthening the negative moment region of continuous T beam. He focused in the negative moment region because it is a critical region due to the interaction of maximum moment and shear.

Alnatit (2011) described the computational study on shear strengthening of reinforced continuous beams using CFRP strips. The study was done through simulation by ABAQUS Software.

Saleh and Barem (2013) were studied the effect of including type of end support, location of the CFRP sheets and type of end anchorage for CFRP. They were found that the externally strengthened continuous reinforced concrete beams with bonded CFRP sheets revealed significant increases in their ultimate loads. Finite element analysis was employed to achieve this study.

Ghasemi et al. (2015) conducted an experimental study on the flexural behavior of continuous unbonded posttensioned HSC beams strengthened using near surface mounted

* *Lecturer Dr. Hayder H. H. Kamonna, University of Kufa\ College of Engineering \ Civil Department \ E-mail: kamonnahh@yahoo.com*

(NSM) and EBR CFRP in both hogging and sagging regions. The results showed that both service and ultimate states of such beams were considerably improved, and also that the efficiency of the NSM method is greater than that of the EBR method, especially in crack propagation and ultimate load.

This work aimed to simulate behavior of continuous reinforced concrete beams strengthened against shear using FRP EBR sheets. Normal and high strength concrete are considered. The range in improvement of shear strength due to prestressing of CFRP sheet (suggested to be added in present work) has been investigated.

2 Description of Test Specimens

Nine full-scale, two-span, continuous reinforced concrete beams, which tested by Khalifa et al. (1999), are investigated. Beams cross section and reinforcement details are shown in Fig. (1). and the mechanical properties of the materials are listed in Table 1. They were grouped into three series labeled CW, CO, and CF, Fig. (1). Series CF is considered as high strength concrete while the two others, CW and CO, are of normal strength. From each series, one beam (CW1, CO1, and CF1) was not strengthened and considered as a reference beam, whereas six beams were strengthened with externally bonded CFRP sheets. Details of all series and test setup as described by Khalifa et al. are mentioned below (Fig. 2).

Series CW consists of two beams (the reference CW1 and CW2). Beam CW2 was strengthened with two CFRP plies. Plies were having perpendicular fiber directions (90°/0°). The first ply was attached in the form of continuous U-wrap with fiber direction oriented perpendicular to the longitudinal axis of the beam (90°). The second ply was bonded to the two sides of the beam with fiber direction parallel to the beam axis (0°).

Three beams were examined in **Series CO**, these are the reference one (CO1), beam CO2 and beam CO3. Beam CO2 strengthened with one-ply CFRP strips in the form of a U-wrap with 90° fiber orientation. The width of the strip was 50 mm. They were spaced 125 mm center to center. Beam CO3 was strengthened with one-ply continuous U-wrap.

Series CF involves four beams, which are reference beam CF1, CF2, CF3 and CF4 beams. For beam CF2, it was strengthened using one-ply continuous U-wrap. In Beam CF3 two CFRP plies having perpendicular fiber directions (90°/0°) were used. Beam CF4 was strengthened using totally wrapped with one-ply CFRP sheets. All beams of this series have no shear reinforcement.

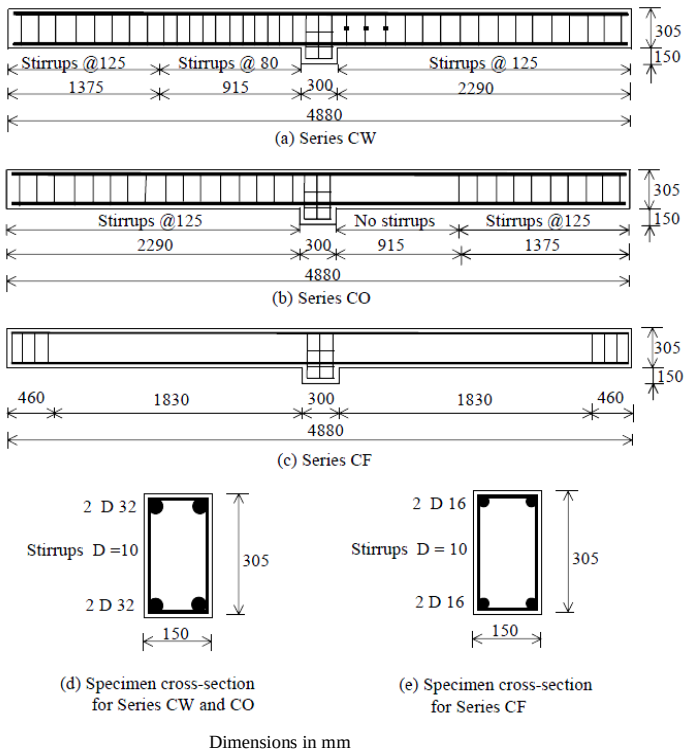

Figure (1) Beam specimens detailing and dimensions (Khalifa et al. 1999)

TABLE 1 – MATERIALS PROPERTIES (KHALIFA ET AL. 1999)

Material	Specifications	Compressive strength (MPa)	Yield point (MPa)	Ultimate tensile strength (MPa)	Modulus of elasticity (GPa)
Concrete	Series CW	27.5	-----	-----	25
	Series CO	20.5	-----	-----	22
	Series CF	50	-----	-----	33
Steel	D = 32 mm	-----	460	730	200
	D = 16 mm	-----	430	700	200
	D = 10 mm	-----	350	530	200
CFRP	t = 0.165 mm	-----	-----	3500	228

Material properties and Finite Element Idealization

3.1 Material Modeling

Concrete in compression behaves as linear-elastic before cracking. At the onset of cracking, a new behavior arises.

In this work elasto-plastic work hardening model followed by a perfectly plastic response is used to simulate the behavior of concrete in compression as shown in Fig.(3) (Willam and Warnke, 1975) .

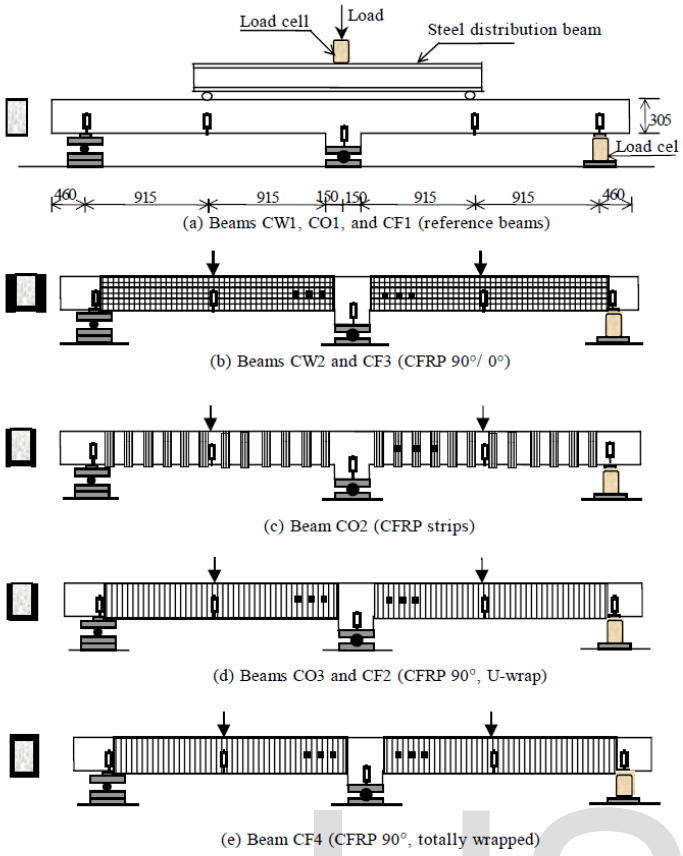

Figure (2) Test set-up and strengthening schemes (Khalifa et al. 1999)

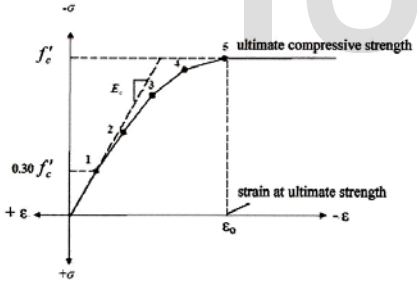

Figure (3) Idealized uniaxial stress-strain curve for concrete (Willam and Warnke, 1975)

The tension stiffening model that shown in Fig. (4) is adopted to represent concrete in tension. The tension stiffening factor, (α_m) was assumed 0.6 (SAS ANSYS 15, 2014).

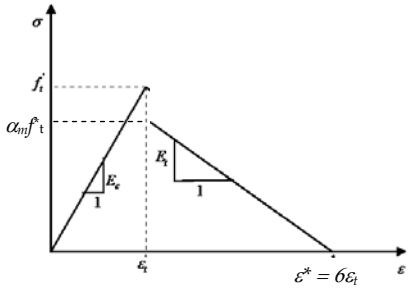

Figure (4) Tension Stiffening Model

For steel bar, that is loaded axially, the behavior is defined as bilinear stress-strain curve as revealed in Fig. (5).

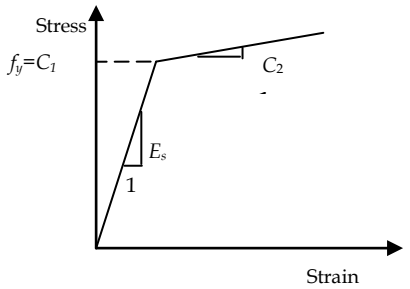

Figure (5) Typical stress strain for steel bar

While a linear elastic orthotropic properties of the FRP composite are assumed throughout this work as displayed in Fig. (6). In addition, perfect bond is assumed between the concrete and CFRPs.

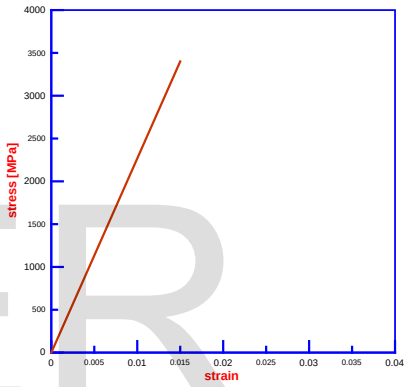

Figure (6) Stress-strain relationship for FRP composite

3.2 Finite Element Idealization

Concrete was modeled using an eight node, SOLID65 element. In this element, Cracking and crushing are permitted in three orthogonal directions at each integration point. Steel reinforcements (shear and longitudinal bars) are represented by a spar LINK180 element. The spar element is a uniaxial tension-compression element. An eight node solid element, SOLID185, is adopted for steel supports and under applied loads. A four node SHELL41 element is used to model CFRP strips. SHELL41 has membrane (in-plane) stiffness but no bending (out-of-plane) stiffness. The element can have variable thickness, large deflection and stress stiffening. All the adopted elements are three dimensional elements having three degrees of freedom at each node; they are translations in the x, y, and z directions (SAS ANSYS 15, 2014).

Making use of symmetry of the tested beam, only one half of beam is used for modeling. Figs. (7) and (8) describe the mesh density, boundary condition, steel plates under loads and at the supports and reinforcement erection for beams that used in the present study.

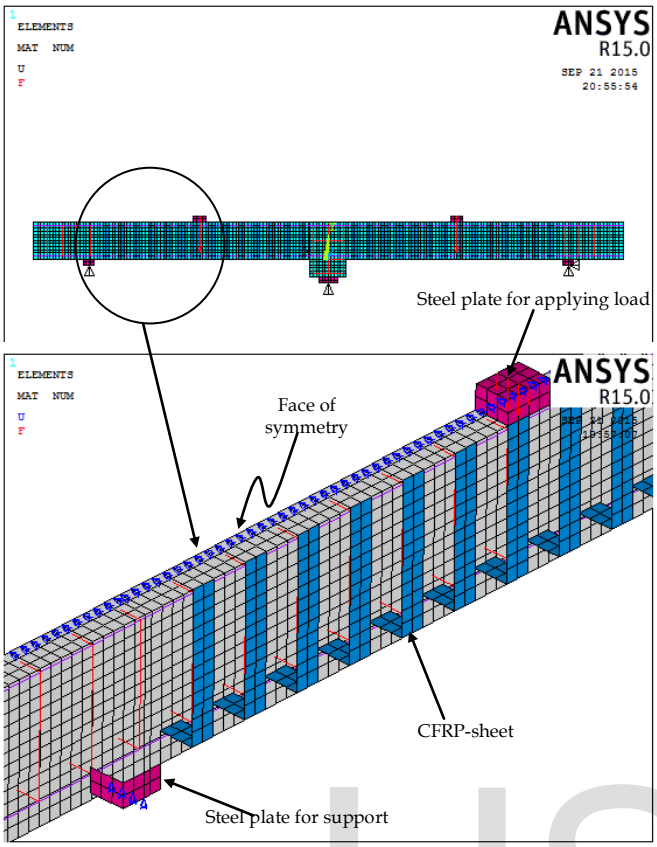

Figure (7) Mesh of the Concrete, Steel Plate, Steel Support and Boundary Conditions for beams.

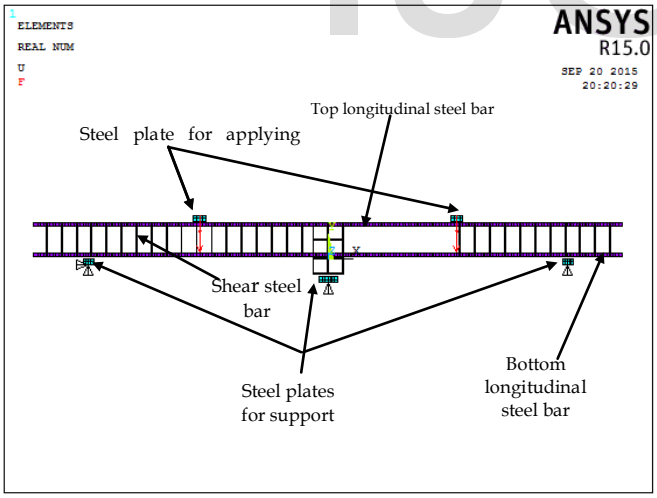

Figure (8) Steel Plate, Steel Support and Reinforcement Configuration for beams

4 Discussion of Results

The three series considered in the present work are discussed separately. The discussion focuses on the shear force-deflection curves and ultimate shear force.

4.1 Series CW

The shear force-deflection curves for specimens of this series (CW1 and CW2) are illustrated in Figs. (9) and (10) respectively. Acceptable agreement between the experimental and numerical results can be seen. The maximum shear force for both beams is found to be (98.8%) and (97.2) from the experimental tests respectively, see Table 2.

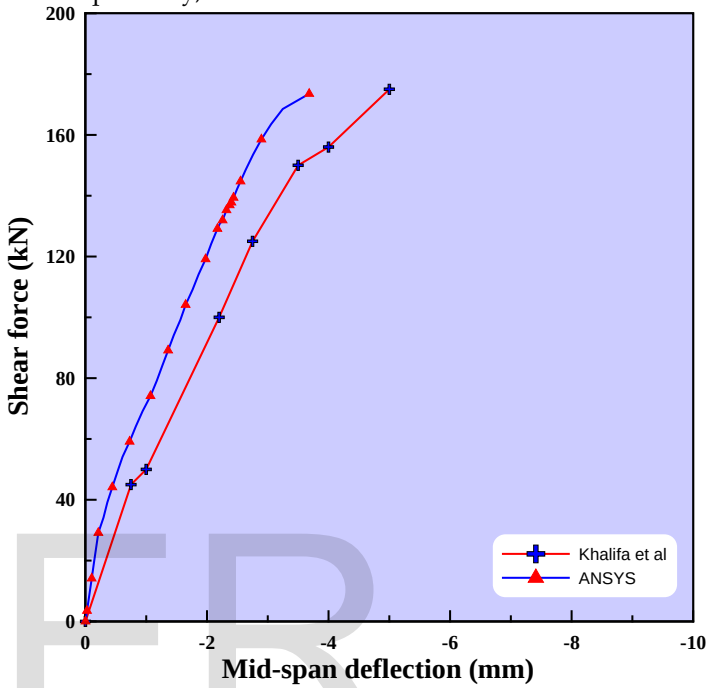

Figure (9) Shear force versus mid-span deflection for beam CW1

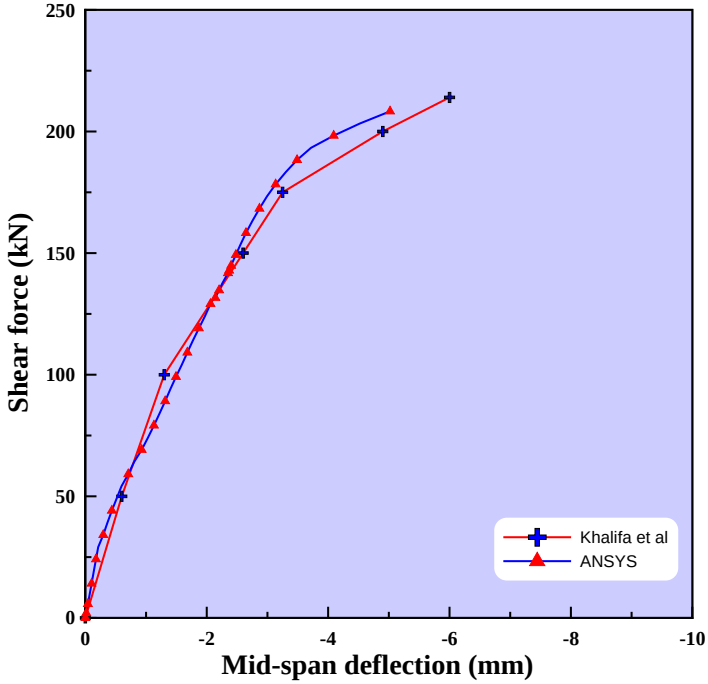

Figure (10) Shear force versus mid-span deflection for beam CW2

4.2 Series CO

Figs. (11), (12) and (13) show the shear force-deflection curves of beams CO1, CO2 and CO3 respectively. It can be simply realized that the numerical results are in a good agreement with the experimental tests. The percentage difference of numerical to experimental failure force are about (0.4%), (0.41%) and (0.9%) for CO1, CO2 and CO3 respectively.

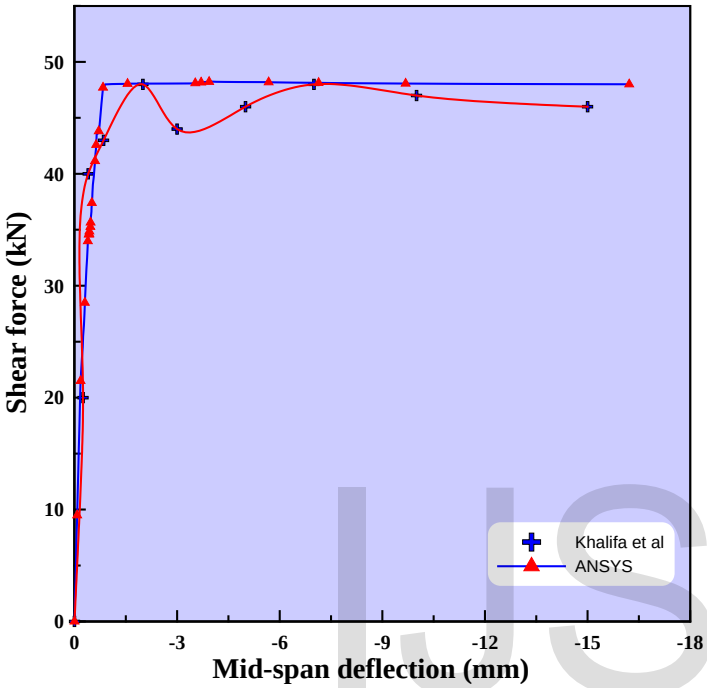

Figure (11) Shear force versus mid-span deflection for beam CO1

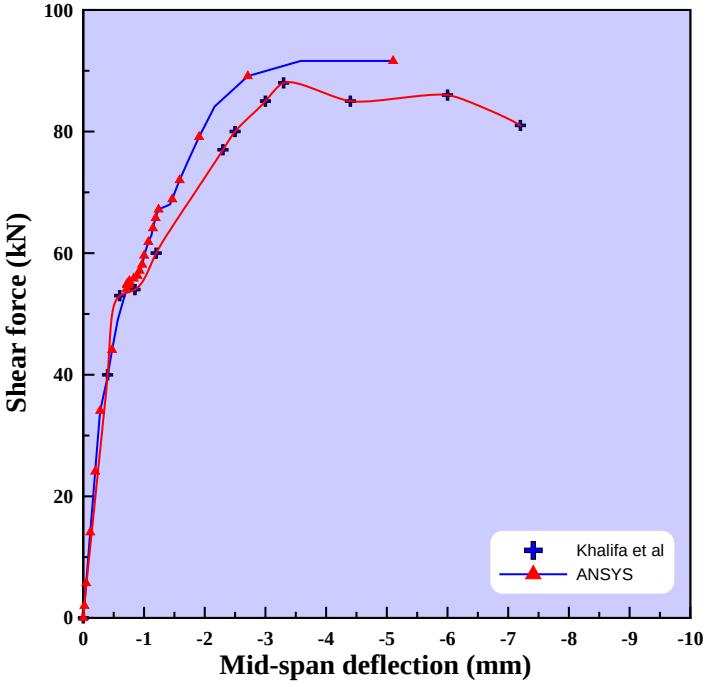

Figure (12) Shear force versus mid-span deflection for beam CO2

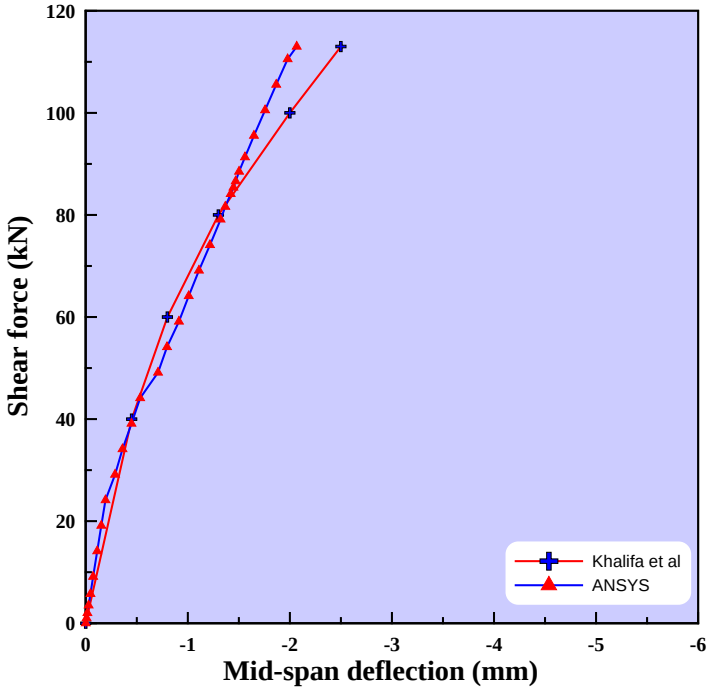

Figure (13) Shear force versus mid-span deflection for beam CO3

4.3 Series CF

The results of beams of this series are illustrated in Figs. (14) to (17). It can be concluded that full shear force-deflection curves with good agreement with experimental results can be achieved. The maximum difference in ultimate shear force, as a ratio of that experimentally recorded, are about (0.3%), (3.6%), (0.8%) and (7.86%) for CF1, CF2, CF3 and CF4 respectively.

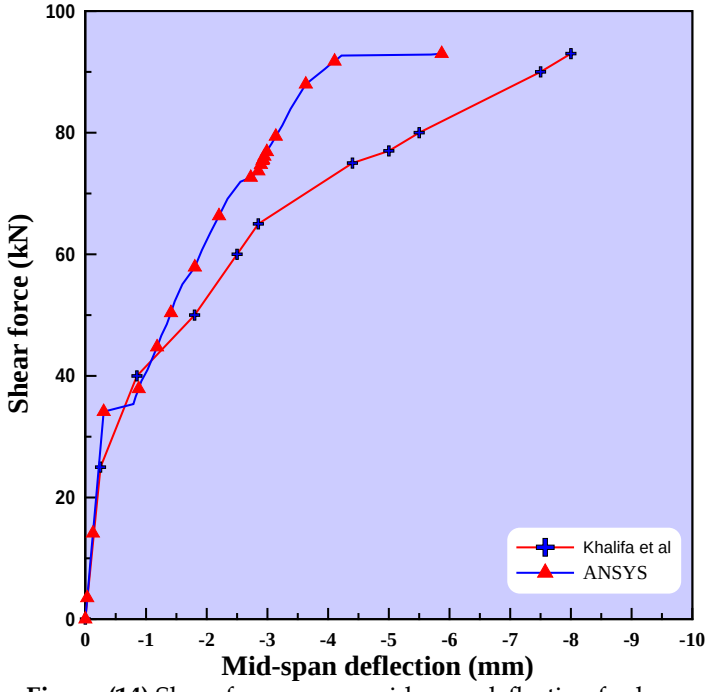

Figure (14) Shear force versus mid-span deflection for beam CF1

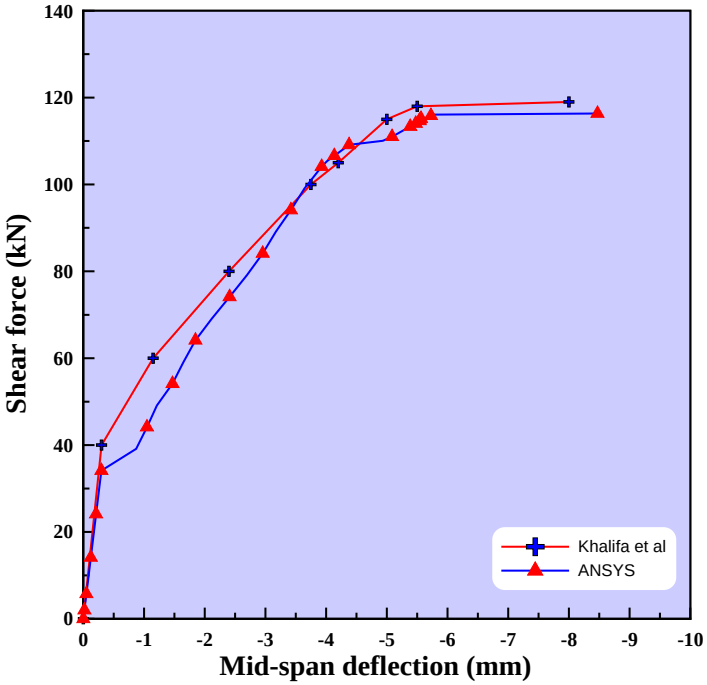

Figure (15) Shear force versus mid-span deflection for beam CF2

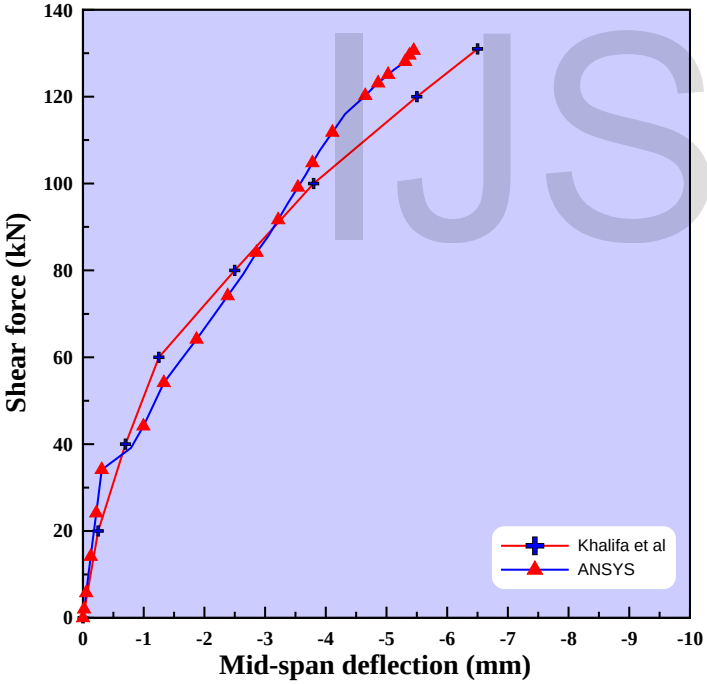

Figure (16) Shear force versus mid-span deflection for beam CF3

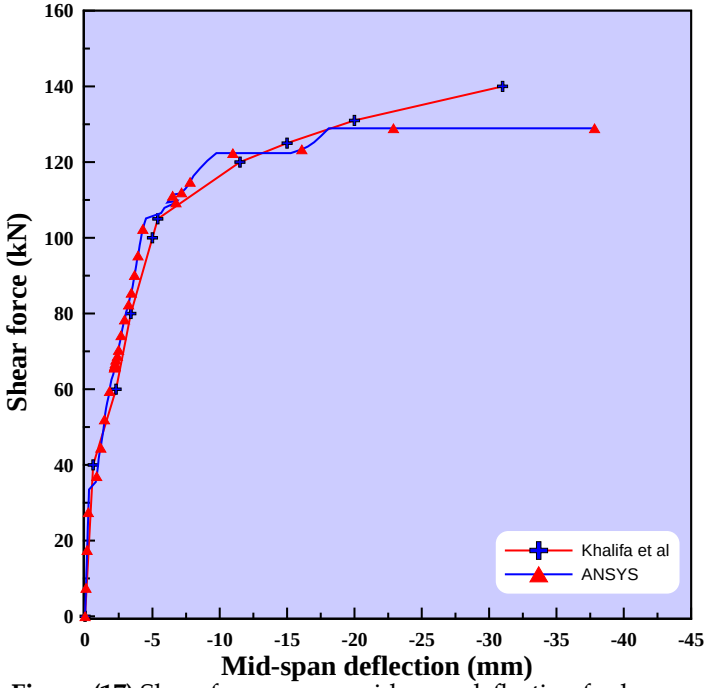

Figure (17) Shear force versus mid-span deflection for beam CF4

Due to present analysis, it is found that most strengthened beams followed stiffer bath in the initial and final stages of loading if compared with the experimental tests. This can be attributed to several causes as, the initial micro-cracks in concrete, no slip assumption between steel and concrete, full bond between concrete and CFRP sheet.

TABLE (2)

COMPARISON BETWEEN EXPERIMENTAL AND THEORETICAL RESULTS

Beam designation		Numerical ultimate shear force (kN)	Experimental ultimate shear force (kN)	V_{num}/V_{exp}
CW-series	CW1	173	175	98.8
	CW2	208	214	97.2
CO-series	CO1	48.18	48	1.004
	CO2	91.6	88	1.041
	CO3	114	113	1.009
CF-series	CF1	92.8	93	99.785
	CF2	116	119	97.479
	CF3	130	131	99.236
	CF4	129	140	92.14

Parametric Studies

As it is well-known that high strength concrete beam is more convenient to achieve prestressing and that beam with no stirrup is weak in shear, thus one specimen of CF series, CF4, is considered in the present study.

Several parameters that associated with effect of prestress on the general response of continuous RC beams initially strengthened by CFRP sheets (in terms of the cracking and ultimate loads) are investigated. These parameters are pre-

stress level, position of prestressed sheets and length of such sheets.

Three longitudinal CFRP sheets are added for applying prestress force. Two are positioned at the bottom face near mid-span of beam while the third one is located at the top face around the interior support, see Fig. (18).

In this study, the application of loads is achieved with two load steps. Prestressing force is applied as the first load step, which uniformly distributed on the nodes attached the longitudinal CFRP sheets, while the second load step includes the application of the vertical load.

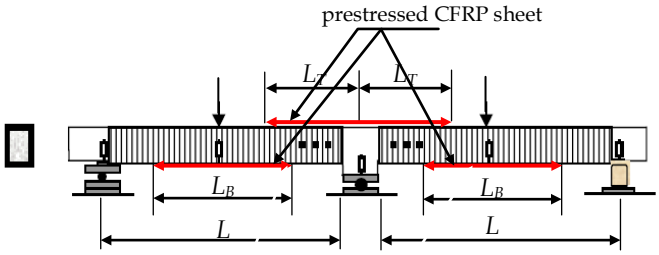

Figure (18) Beam CF4 with added prestressed longitudinal CFRP sheets

5.1 Effect of prestressing ratio

As it is mentioned above, the influence of using different prestressing level on the behavior of continuous RC beam is examined. Prestressing is applied at both top sheets (with proposed length of L_T= 0.35L) and bottom sheets (with length of L_B = 0.5L). Where L_T is half length of top sheet, L_B is length of each one bottom sheets and L is unsupported length of beam, see Fig. (18). Four ratios of prestressing force to the tensile strength of CFRP sheet are chosen, which are (0%, 20%, 35% and 50%). These are the same values suggested by Shang et al. (2005). Prestressing ratio greater than 50% does not be considered to avoid debonding problems (Shang et al. 2005).

Fig. (19) shows the load deflection curves with different prestress levels. It is obvious that ultimate load increases with adopting more values of prestress force on the added CFRP sheets. It is simply realized that, the increment is reduced with increasing prestress value, see Figs. (19) and (20). Also this figure yielded that the cracking load increases with this parameter following a path very close to be linear. This may be attributed to that the prestressed sheets resist the external loads in the early stages of loading. More contributions in resistance may be expected with progress of load application.

It can be seen that an improvement in cracking and ultimate loads of about 89 %and 36%, respectively, when prestressing level increased up to 50%.

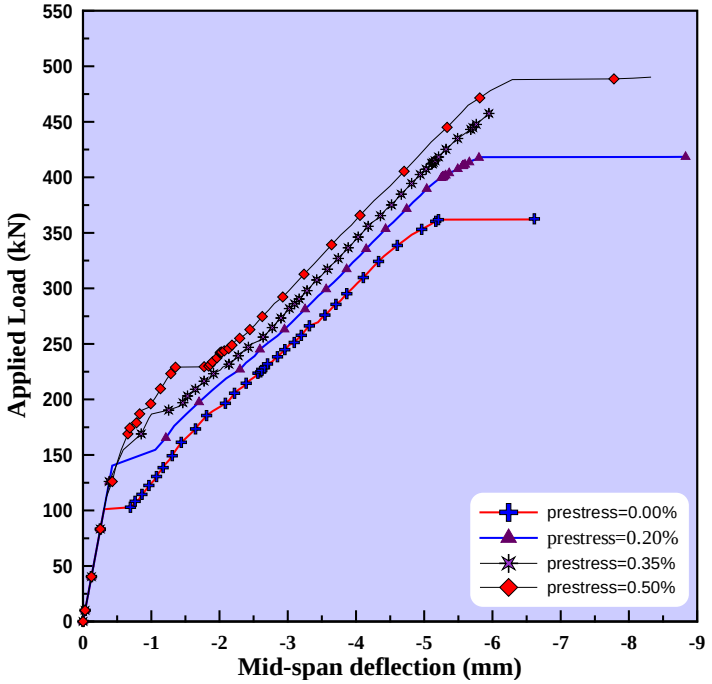

Figure (19) Effect of prestressing ratio in the load deflection curves

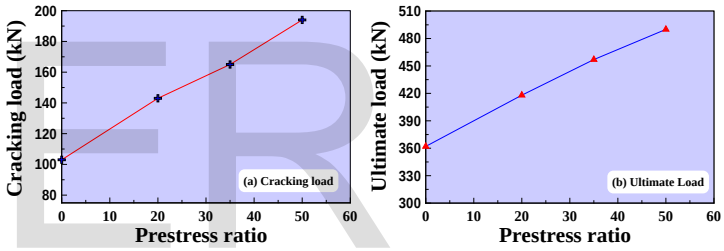

Figure (20) Effect of prestressing ratio in the cracking and ultimate loads

5.2 Effect of position of CFRP sheets to be prestressed

To show the effect of position of CFRP sheets to be prestressed, the prestress is applied on such sheets in a predetermined configuration (no prestressing at all sheets, at bottom CFRP sheets only, at top CFRP sheet only and at both bottom and top CFRP sheets). The range of influence of this parameter can be found in Fig. (21). It can be noted that prestressing of bottom sheets (in the positive moment region) has more effect on the response than prestressing of top sheet (in the negative moment region). This is may be attributed to the difference in degree of restraining against vertical movement in regions of positive and negative moment. This may affect the camber value caused by prestressing stage. An increments of the cracking and ultimate loads of about 21% and 24%, respectively, are obtained when prestressing force is applied at bottom CFRP sheets compared with no prestressing case. While prestressing the top sheet shows an increment of about 10% and 7% for cracking and ultimate loads respectively. Also, it seems that applying prestress force on bottom sheets yield

relatively good performance in comparison with the other arrangements of prestressing if the cost of sheet installation is taken in consideration.

The effect of which sheet has to be prestressed on the cracking and ultimate loads are stated in Fig. (22). This figure reveals that the largest value of cracking load can be obtained when adopting any one of the last two configurations. Thus, the third manner of prestress application is recommended due to the economy view.

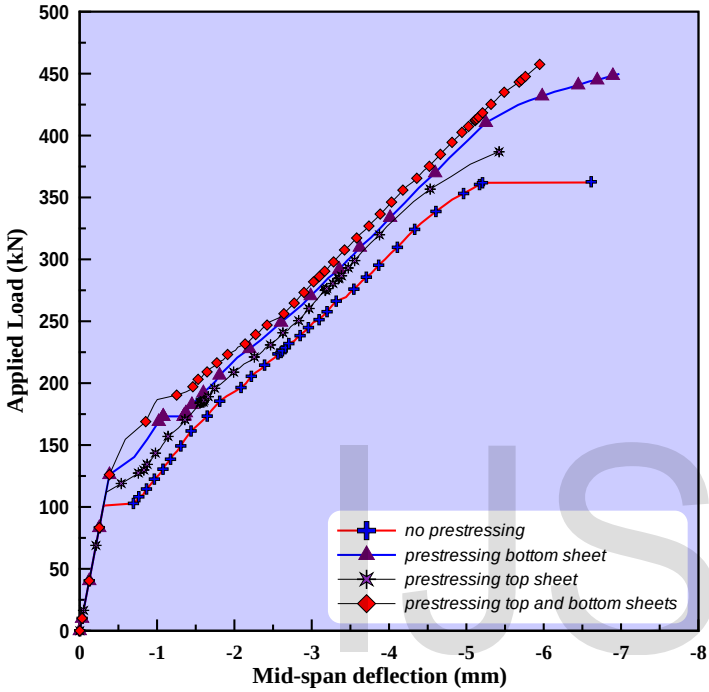

Figure (21) Effect of prestressing position on the load deflection curves

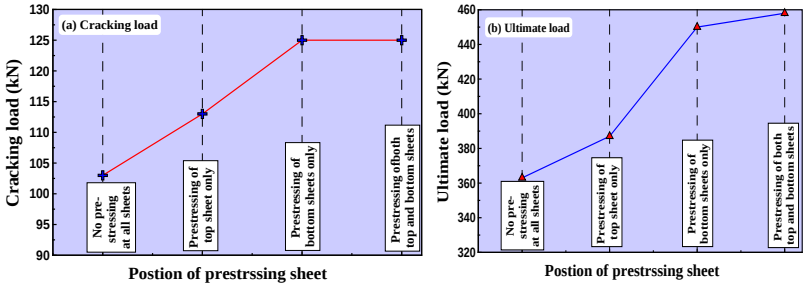

Figure (22) Effect of prestressing position on the cracking and ultimate loads

5.3 Effect of the length of prestressing sheets

Length of prestressing CFRP sheets along top and bottom faces of beam influence is also considered. The effect of length of either top or bottom sheets is studied separately.

5.3.1 **Effect of the length of bottom sheet**s

To study the effect of this parameter, the same beam CF4 with the added sheets is investigated. Here the length of the added bottom sheets is changed in equal intervals (L_B = 0.25L, 0.5L, 0.75L and 1.0L). While, the bottom sheet length is kept constant (L_T = 0.35L).

The load deflection curves are shown Fig. (23). It can be noted that there is some effect of variation of sheet length on the overall response. Also, it is obvious that the recorded cracking load is affected considerably in the range of (0.25L-0.75L) as shown in Fig. (24). Beyond this (full length), the cracking load is unchanged. This may be due to the fact that the continuous beam is subjected to negative moments in region between interior support and inflection points. Thus extending sheet to this region eliminates its activity. It is found that adopting bottom sheet length of (L_B=0.75L) results in an increment of the cracking load of about 43% rather than a sheet of length 0.25L.

Also it can be seen that the ultimate load continue to be improved for ($L_B \geq 0.75L$). It is found that using sheet of length equal to one span rather than a sheet of one-fourth of span results in 11%. This may be caused due to the redistribution of moments near the interior support. This leads to activate some portions of sheet that where inactive in early stage (zone of negative moments).

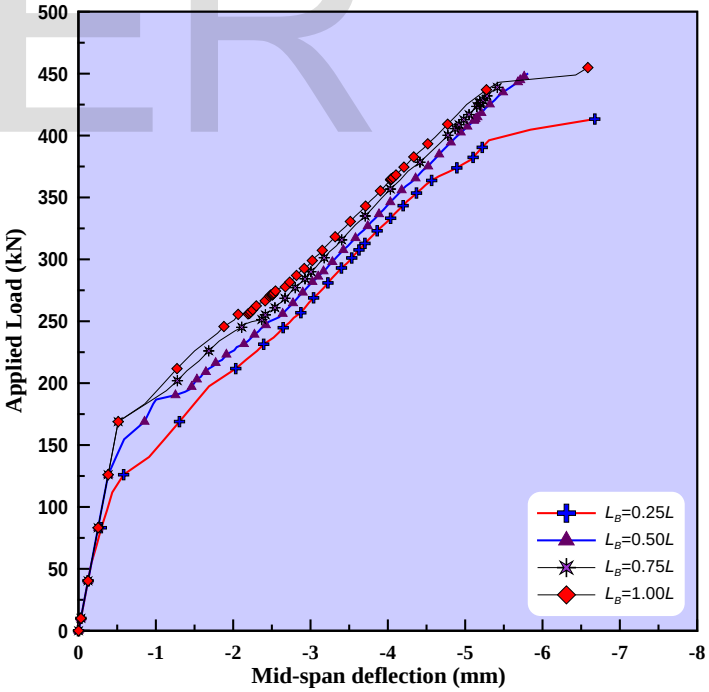

Figure (23) Effect of length of prestressing bottom sheet on the load deflection curves

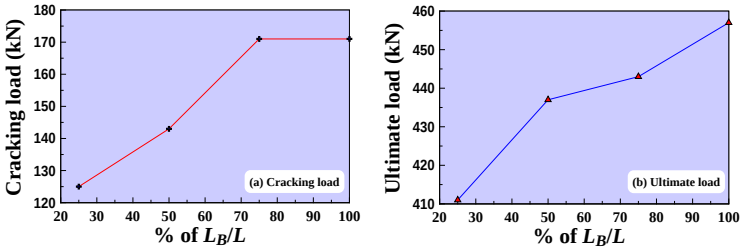

Figure (24) Effect of length of prestressing bottom sheet on the cracking and ultimate loads

5.3.2 **Effect of the length of top prestressing sheet**

Here, Length of prestressed top sheet is changed by about (L_T=0.0L, L_T=0.25L, L_T=0.35L and L_T=0.5L). Whereas bottom sheet length is maintained constant and equal (L_B=0.5L). Fig. (25) states the load deflection curves of beams. By making a comparison between Figs. (23) and (25), it is clear that the length variation of top length has lesser effect on behavior of beam than the bottom sheet. With progress of loading, the inflection point shifts (due to nonlinear behavior) towards the interior support. This may reduce the zone that the top sheet may be active. This shifting has less effect on performance bottom sheet with the same stages of loading. From Fig. (26), it can be also observed that the improvement on the behavior of beam is reduced or stopped as sheet length be (L_T > 0.25L), i.e. beyond the inflection point. The ultimate load begins to be dropped as (L_T > 0.35L). This may due to the interaction effects of prestressing with the vertical forces.

So it is not recommended to extend the prestressed CFRP sheet beyond inflection point if improvement of RC continuous beam is aimed.

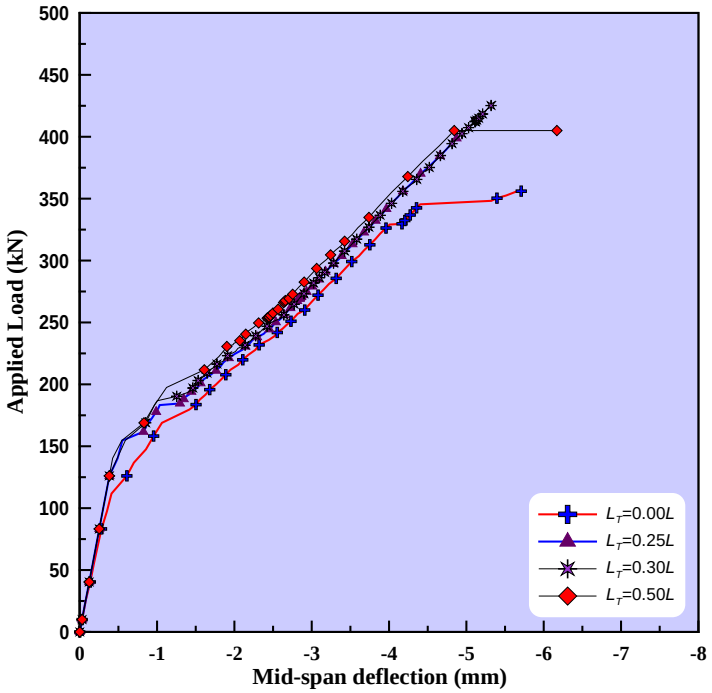

Figure (25) Effect of length of prestressing top sheet on the load deflection curves

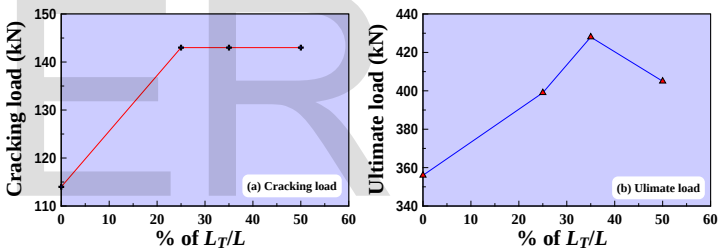

Figure (26) Effect of length of prestressing top sheet on the cracking and ultimate loads

6 Conclusions

This work is primarily concerned with studying the effect of prestress on the behavior of continuous RC beams strengthened CFRP sheets. The following conclusions can be drawn:

1. Good simulation can be obtained by using ANSYS program for RC continuous beams strengthened by CFRP sheets with maximum devotion in ultimate shear force of 8% from the experimental results.
2. Prestress level on suggested CFRP sheets has a considerable effect on cracking and ultimate loads. Those were increased by about 89% and 36%, respectively, when prestressing force ratio increases up to 50%.
3. The relationship obtained between the prestressing ratio and cracking load is close to be linear.
4. Changing the length of prestressing CFRP sheets in the top face has lesser effect than those in the bottom face due to presence of support in the negative mo-

ment region, which restricted occurring of camber.

5. It is found that the extension of CFRP sheets beyond the inflection point has a reverse action on the beam performance.
6. Prestressing of top CFRP sheet may be considered less effective and uneconomic compared with bottom CFRP sheets.

7 REFERENCES

[1] Alnatit, N. M. E., (2011)," Computational Study on Shear Strengthening of RC Continuous Beams Using CFRP Sheet "M. Sc. Thesis, Tun Hussein Onn Malaysia.

[2] Ashour A. F., El-Refaie S. A., Garrity S. W. (2004). "Flexural strengthening ofRC continuous beams using CFRP laminates", Cem Concr Compos.26: 765-75.

[3] Ghasemi, S., Maghsoudi, A., Bengar, A. H., and Ronagh, R. H., (2015). "Sagging and Hogging Strengthening of Continuous Unbonded Posttensioned HSC Beams by NSM and EBR." J. Compos. Constr. , 10.1061/(ASCE).

[4] Grace, N. F., (2001) "Strengthening of negative moment region of RC beams using CFRP Strips". ACI structural journal. Vol 98.

[5] Jumaat, M. Z., Rahman, M. M and Alam, M. A. (2010)," Flexural strengthening of RC continuous T beam using CFRP laminate: A review", International Journal of the Physical Sciences Vol. 5(6), pp. 619-625.

[6] Khalifa, A., Tumialan, G., Nanni, A. and Belarbi, A., (Nov. 1999)"Shear Strengthening of Continuous RC Beams Using Externally Bonded CFRP Sheets," SP-188, American Concrete Institute, Proc., 4th International Symposium on FRP for Reinforcement of Concrete Structures (FRPRCS4), Baltimore, MD, pp. 995-1008.

[7] Maghsoudi, A.A., Bengar H. (2009). Moment redistribution and ductility of RHSC continuous beams strengthened with CFRP. Turkish J. Eng. Env. Sci. 33: 45-59.

[8] Saleh, A. R. and Barem, A. A. H.,(2013)," Experimental and Theoretical Analysis for Behavior of R.C. Continuous Beams Strengthened by CFRP Laminates "Journal of Babylon University, Engineering Sciences, No.(5), Vol.(21), PP. 1555-1567.

[9] SAS ANSYS 15, (2014), "Finite Element Analysis System", SAS IP, Inc., U.S.A.

[10] Shang, S., Zou P. X.W., Peng, H. and Wang, H., "Avoiding De-Bonding in FRP Strengthened Reinforced Concrete Beams Using Prestressing Techniques", Proceedings of the International Symposium on Bond Behaviour of FRP in Structures (BBFS 2005).

[11] Taerwe, L. Vasseur, L. and Matthys S.,(2009)," External strengthening of continuous beams with CFRP" Concrete Repair, Rehabilitation and Retrofitting II – Alexander et al (eds), Taylor & Francis Group, London, pp. 43-53.

[12] Willam, K. J., and Warnke, E. P., "Constitutive Model for Triaxial Behavior of Concrete", Seminar on Concrete Structures Subject to Triaxial Stresses", International Association of Bridge and Structural Engineering Conference, Bergamo, Italy, 1974, 174 pages.

8 LIST OF SYMBOLS

C_1	Constant Represent Yield Strength of Steel
C_2	Constant Represent Strain Hardening of Steel
CF	Third Series of RC Continuous beams
CFRP	Carbon Fiber Reinforced Polymer
CO	Second Series of RC Continuous beams
CW	First Series of RC Continuous beams
EBR	Externally Bonded Reinforcement
f'_c	Ultimate Strength of Concrete in Compression
f_t	Ultimate Strength of Concrete in Tension
f_y	Yield Strength of Steel
L	Length of Unsupported Length of Beam
L_B	Length of Prestressed CFRB Sheet in the Bottom Face Beam
L_T	Length of Prestressed CFRB Sheet in the Top Face of Beam
NSM	Near Surface Mounted
RC	Reinforced Concrete
RHSC	Reinforced High Strength Concrete
V_{exp}	Ultimate Shear Force Obtained by Experimental Test
V_{num}	Ultimate Shear Force Obtained by Finite Element Analysis
E_c	Modulus of Elasticity of Concrete in Compression
E_s	Modulus of Elasticity of Steel
E_t	Slope of Descending part of Stress- Strain Curve of Concrete in Tension
ε_o	Ultimate Strain of Concrete in Compression
ε_t	Tensile Strain of Concrete at Onset of Cracking of concrete in Tension
ε^*	Ultimate Strain of Concrete in Tension